Article

A magnetar giant flare in the nearby starburst galaxy M82

https://doi.org/10.1038/s41586-024-07285-4

Received: 22 December 2023

Accepted: 7 March 2024

Published online: 24 April 2024

Check for updates

Sandro Mereghetti[1]✉, Michela Rigoselli[1], Ruben Salvaterra[1], Dominik Patryk Pacholski[1,2], James Craig Rodi[3], Diego Gotz[4], Edoardo Arrigoni[1,5], Paolo D'Avanzo[6], Christophe Adami[7], Angela Bazzano[3], Enrico Bozzo[8,9], Riccardo Brivio[6,10], Sergio Campana[6], Enrico Cappellaro[11], Jerome Chenevez[12], Fiore De Luise[13], Lorenzo Ducci[8,14], Paolo Esposito[1,15], Carlo Ferrigno[6,8], Matteo Ferro[6,10], Gian Luca Israel[9], Emeric Le Floc'h[4], Antonio Martin-Carrillo[16], Francesca Onori[13], Nanda Rea[17,18], Andrea Reguitti[6,11], Volodymyr Savchenko[8,19], Damya Souami[20], Leonardo Tartaglia[13], William Thuillot[21], Andrea Tiengo[1,15], Lina Tomasella[11], Martin Topinka[22], Damien Turpin[4] & Pietro Ubertini[3]

Magnetar giant flares are rare explosive events releasing up to 10^{47} erg in gamma rays in less than 1 second from young neutron stars with magnetic fields up to $10^{15–16}$ G (refs. 1,2). Only three such flares have been seen from magnetars in our Galaxy[3,4] and in the Large Magellanic Cloud[5] in roughly 50 years. This small sample can be enlarged by the discovery of extragalactic events, as for a fraction of a second giant flares reach luminosities above 10^{46} erg s^{-1}, which makes them visible up to a few tens of megaparsecs. However, at these distances they are difficult to distinguish from short gamma-ray bursts (GRBs); much more distant and energetic ($10^{50–53}$ erg) events, originating in compact binary mergers[6]. A few short GRBs have been proposed[7–11], with different amounts of confidence, as candidate giant magnetar flares in nearby galaxies. Here we report observations of GRB 231115A, positionally coincident with the starburst galaxy M82 (ref. 12). Its spectral properties, along with the length of the burst, the limits on its X-ray and optical counterparts obtained within a few hours, and the lack of a gravitational wave signal, unambiguously qualify this burst as a giant flare from a magnetar in M82.

Instruments on board the INTEGRAL satellite detected gamma-ray burst (GRB) 231115A on 15 November 2023 at 15 h 36 min 20.7 s Universal Time (UT) (ref. 13). This short burst (duration T_{90} = 93 ms) was seen also by other satellites[14–18], but only INTEGRAL could promptly associate it to M82 thanks to a localization at the level of a few arcmin, publicly distributed by the INTEGRAL Burst Alert System[19] only 13 s after the burst detection. The burst occurred in the field of view of the IBIS coded mask instrument[20], at the following coordinates: right ascension (RA) 9 h 56 min 05 s, declination (dec.) +69° 40′ 19″ (J2000, 2 arcmin 90% confidence level radius). This position is consistent with, and supersedes, the one derived using the preliminary satellite attitude available in near real time[13]. The position of GRB 231115A coincides with the nearby starburst galaxy M82 (ref. 12) (Fig. 1). Notably, the central region of the galaxy, where most star formation activity occurred, is inside the INTEGRAL–IBIS error region. Considering that the total angular size of all the galaxies with apparent luminosity brighter than M82 (excluding the Magellanic Clouds and M31) is roughly 6,000 arcmin^2, the chance alignment with GRB 231115A is 4×10^{-5}. A more elaborate analysis[21] indicates that the Bayes factor favouring a giant flare in M82 with respect to a chance alignment of a short GRB in the background is a factor 30 larger than that of the previous best candidate (GRB 200415A possibly associated to NGC 253 (ref. 9)), making GRB 231115A by far the most compelling case for a giant flare from a magnetar outside the local group of galaxies. Although strong evidence for an extragalactic population of giant flares emerged from a joint statistical analysis of the previous candidates[10], here we rapidly identify a giant magnetar flare and securely associate it with a nearby galaxy, thanks to a precise localization obtained in near real time.

The light curves plotted in Fig. 2 show that GRB 231115A was clearly visible in the two IBIS detectors, which operate in different energy ranges: ISGRI (the INTEGRAL soft gamma-ray imager)[22] (20 keV–1 MeV) and PICsIT (pixellated imaging CsI telescope)[23] (175 keV–15 MeV). The ISGRI and PICsIT spectra of the burst, extracted from the time interval with a significant detection in both detectors (from T_0 + 0.687 to

[1]INAF - Istituto di Astrofisica Spaziale e Fisica Cosmica di Milano, Milano, Italy. [2]Dipartimento di Fisica G. Occhialini, Università degli Studi di Milano Bicocca, Milan, Italy. [3]INAF - Istituto di Astrofisica e Planetologia Spaziali di Roma, Rome, Italy. [4]Université Paris-Saclay, Université Paris Cité, CEA, CNRS, AIM, Gif-sur-Yvette, France. [5]Dipartimento di Fisica, Università degli Studi di Milano, Milan, Italy. [6]INAF - Osservatorio Astronomico di Brera, Merate, Italy. [7]Aix-Marseille Univ., CNRS, CNES, LAM, Marseille, France. [8]University of Geneva, Department of Astronomy, Versoix, Switzerland. [9]INAF - Osservatorio Astronomico di Roma, Monte Porzio Catone, Italy. [10]Dipartimento di Scienza e Alta Tecnologia, Università dell'Insubria, Como, Italy. [11]INAF - Osservatorio Astronomico di Padova, Padova, Italy. [12]DTU Space, Technical University of Denmark, Kongens Lyngby, Denmark. [13]INAF - Osservatorio Astronomico d'Abruzzo, Teramo, Italy. [14]Institut fuer Astronomie und Astrophysik Tuebingen, Tuebingen, Germany. [15]Scuola Universitaria Superiore IUSS Pavia, Pavia, Italy. [16]School of Physics and Centre for Space Research, University College Dublin, Belfield, Dublin, Ireland. [17]Institute of Space Sciences (ICE-CSIC), Campus UAB, Barcelona, Spain. [18]Institut d'Estudis Espacials de Catalunya, Barcelona, Spain. [19]École polytechnique fédérale de Lausanne, Lausanne, Switzerland. [20]LESIA, Observatoire de Paris, Université PSL, CNRS, Sorbonne Université, Université de Paris, Meudon, France. [21]Institut de mecanique celeste et de calcul des ephemerides (IMCCE) UMR 8028 du CNRS - Observatoire de Paris, Université PSL, Paris, France. [22]INAF - Osservatorio Astronomico di Cagliari, Selargius (CA), Italy. ✉e-mail: sandro.mereghetti@inaf.it

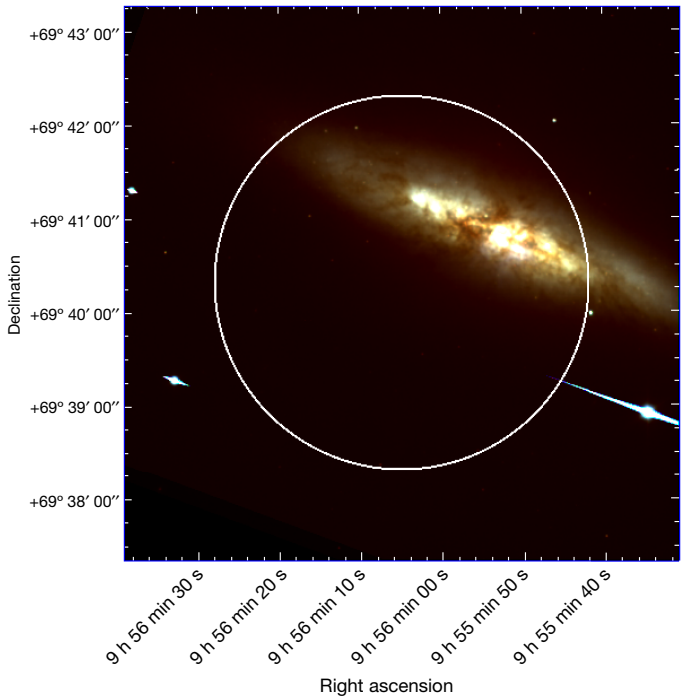

Fig. 1 | Optical image of M82. Created from data obtained with the TNG. RGB scale: z band, red; i band, green; r band, blue). The 90% cl error circle of GRB 231115A has a radius of 2 arcmin.

T_0 + 0.748 s, with T_0 = 15 h 36 min 20.0 s UT), have been jointly fit and are well described by an exponentially cut-off power law with photon index $\alpha = 0.04^{+0.27}_{-0.24}$, peak energy $E_p = 551^{+81}_{-59}$ keV and flux $F_{30-2,600} = (7.2^{+0.6}_{-0.7}) \times 10^{-6}$ erg cm^{-2} s^{-1} in the 30 keV–2.6 MeV range (see Methods section 'INTEGRAL data analysis and results'). Assuming this spectral shape for the whole duration of the burst, the fluence in the same energy range is $(6.3 \pm 0.5) \times 10^{-7}$ erg cm^{-2}.

M82 was in the field of view of IBIS starting from 9.2 hours before up to 11.8 min after the occurrence of GRB 231115A, but no other bursts were detected. The corresponding fluence upper limit of the order of 10^{-7} erg cm^{-2} for a 0.1 s duration does not exclude the possibility of precursor activity as seen in the Galactic giant flares[3,4]. An INTEGRAL target of opportunity (ToO) observation was performed in the following 3 days, but no other bursting or persistent emission was detected by IBIS from the direction of M82. Integrating all the data of the ToO observation, we obtained an upper limit of 2.6×10^{-11} erg cm^{-2} s^{-1} on the 30–100 keV persistent emission at the position of GRB 231115A. Also, no other bursts from M82 were detected in all the available ISGRI archival data obtained since 2003, which provided a total exposure of more than 16 Ms (see Methods section 'INTEGRAL data analysis and results').

At the distance of M82 (3.6 Mpc (ref. 24)), the GRB 231115A fluence measured with IBIS implies an emitted isotropic energy $E_{iso} = 10^{45}$ erg (1 keV–10 MeV), well below the typical value for a short GRB, but consistent with the one of the initial pulses of the three giant flares securely associated with magnetars[3–5]. The short duration and hard spectrum of GRB 231115A are also in agreement with the properties seen in the initial pulses of giant flares. In the three giant flares securely associated with magnetars, the initial short and hard pulse was followed by a softer tail, with a duration of a few minutes and a maximum luminosity of roughly 10^{42} erg s^{-1}, characterized by a periodic modulation induced by the neutron star rotation. A similar feature would be too faint to be visible by IBIS at the distance of M82. This is shown in Fig. 3, where we compare the limits obtained for GRB 231115A with the light curve of the most energetic galactic giant flare ever observed (the one emitted by SGR 1806–20 in 2004[4]) rescaled to a distance of 3.6 Mpc.

The field of GRB 231115A was promptly observed with the Neil Gehrels Swift Observatory starting 9 ks after the burst[25] and a deeper X-ray observation was carried out with the XMM-Newton satellite, starting

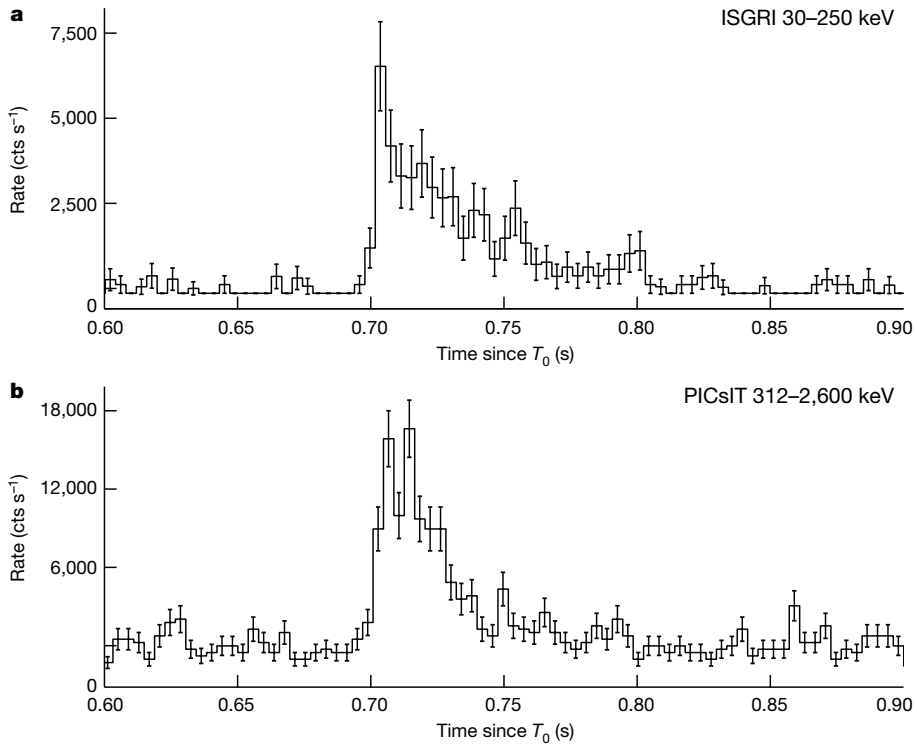

Fig. 2 | Light curves of GRB 231115A. a,**b**, Background-subtracted light curves (errors are at 1σ) obtained with the ISGRI detector in the 30–250 keV energy range (**a**) and with the PICsIT detector in the 312–2,600 keV energy range (**b**). Time refers to T_0 = 15 November 2023 15 h 36 min 20 s UT (time at the INTEGRAL position; the burst reached instruments on low Earth orbit satellites about 0.4 s later).

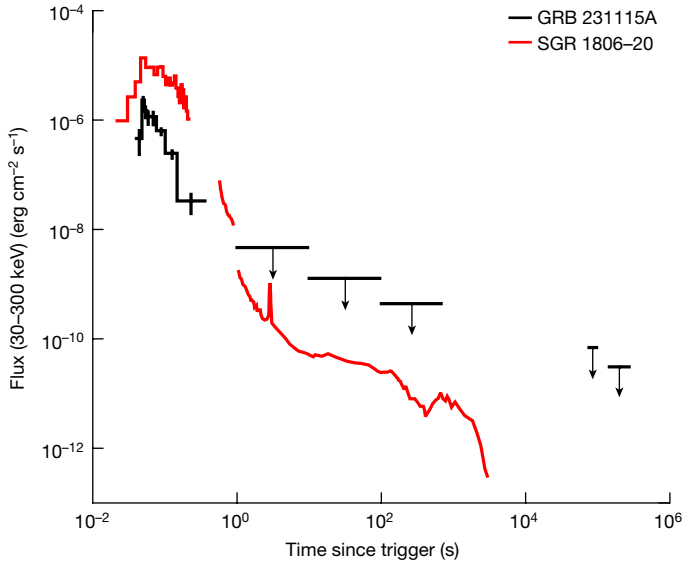

Fig. 3 | Comparison between GRB 231115A and the 2004 giant flare from SGR 1806–20. Errors are at 1σ, upper limits are at 3σ. The light curve of SGR 1806–20 (red) has been rescaled to the distance of M82 (data from Helicon-Coronas-F[34], Konus-Wind[34] and INTEGRAL SPI-ACS[35]). Note that the 5.2 s periodicity in the SGR 1806–20 light curve is not visible due to the used bin size.

0.7 days after the burst[26] (see Methods section 'X-ray observations'). The comparison of the Swift and XMM-Newton images with those obtained in previous observations of M82 does not show evidence for new X-ray sources inside the GRB 231115A error region. Owing to the presence of unresolved X-ray emission from the central part of the galaxy, the corresponding upper limit is position dependent. The limit of 4×10^{-14} erg cm^{-2} s^{-1} derived from the XMM-Newton data, which applies to 60% of the error region, is inconsistent with the flux at $T_0 + 1$ day of most X-ray afterglows of short GRBs detected with the Swift–X-ray telescope (XRT) instrument (Extended Data Fig. 4). Although we cannot exclude a rapid afterglow drop, as observed in the class of so-called short lived short GRBs[27], this X-ray upper limit disfavours the GRB interpretation. It is instead consistent with the quiescent X-ray emission of a magnetar in M82. In fact the X-ray luminosity of known magnetars, also considering the peak values reached during outbursts[28], never exceeds 10^{36} erg s^{-1}, corresponding to 6×10^{-16} erg cm^{-2} s^{-1} at the M82 distance.

Holding true the association of GRB 231115A with M82 on the basis of the remarkable spatial coincidence, the low value of E_{iso} could be reconciled with a short GRB origin only if the jet axis is pointed away from our direction, similar to the case of the gravitational wave event GRB 170817A (ref. 29), which produced the bright kilonova AT2017gfo in the optical or near-infrared band. However, the deep upper limits of $m > 20.0$–24.0 mag (depending on the assumed position in the INTEGRAL error circle) on the optical counterpart that we obtained starting at $T_0 + 0.2$ days (see Methods section 'Optical observations') exclude this possibility, both for an AT2017gfo-like event and for even fainter kilonovae (Extended Data Fig. 5). Furthermore, an off-axis GRB event would probably show a longer duration than that observed for GRB 231115A. We finally note that the binary merger of two compact objects at 3.6 Mpc would have produced a strong signal in gravitational waves, at variance with the non-detection reported by the LIGO–Virgo–KAGRA Collaboration[30].

The discovery of a young, active magnetar in M82, a starburst galaxy characterized by a high star formation rate[31] is consistent with the origin of magnetars in core collapse supernova explosions[32]. The volumetric rate of giant flares with $E_{iso} > 4 \times 10^{44}$ erg has been recently estimated[10] as $(3.8^{+4.0}_{-3.1}) \times 10^5$ Gpc^{-3} yr^{-1}. Assuming a direct link with the young stellar population of core collapse progenitors and considering the total star formation rate of 4,000 $M_\odot$ per year (mass of the Sun per year) within 50 Mpc, this corresponds to a rate of $R(E_{iso} > 4 \times 10^{44}) = 0.05^{+0.05}_{-0.04}$ yr^{-1} $(M_\odot\,\mathrm{yr}^{-1})^{-1}$. Given the star formation rate of 7.1 $M_\odot$ per year in M82 (ref. 31) and assuming a power-law distribution of the giant flares energies with slope 1.7, the expected rate of giant flares with $E_{iso} > 10^{45}$ erg in M82 is $R_{M82}(E_{iso} > 10^{45}) = 0.19^{+0.19}_{-0.15}$ per year. Recent calculations based on relativistic hydrodynamical simulations[33] show that such ejecta are efficient sources for the nucleosynthesis of heavy elements through the r process. Thus the giant flares with $E_{iso} > 10^{46}$ erg (each producing up to 10^{26} g of ejecta) can give a yield of roughly 2×10^{-9} $M_\odot$ per year of r-process elements in M82 through this channel.

GRB 051103 is another short GRB that has been proposed as a possible giant flare from a magnetar in the M81 group of galaxies[7]. According to a detailed statistical analysis[10], M82 is the most likely host of GRB 051103, despite being slightly outside its 260 arcmin^2 localization region. The rate of giant flares derived above is fully consistent with the detection of two events from M82 in 20 years. Therefore, starburst galaxies such as M82, which produce a significant population of young magnetars, seem promising targets to constrain the energy distribution function of giant flares by means of long dedicated observations with future high sensitivity instruments.

Online content

Any methods, additional references, Nature Portfolio reporting summaries, source data, extended data, supplementary information, acknowledgements, peer review information; details of author contributions and competing interests; and statements of data and code availability are available at https://doi.org/10.1038/s41586-024-07285-4.

1. Mereghetti, S. The strongest cosmic magnets: soft gamma-ray repeaters and anomalous X-ray pulsars. *Astron. Astrophys. Rev.* **15**, 225–287 (2008).
2. Kaspi, V. M. & Beloborodov, A. M. Magnetars. *Ann. Rev. Astron. Astrophys.* **55**, 261–301 (2017).
3. Hurley, K. et al. A giant periodic flare from the soft γ-ray repeater SGR1900+14. *Nature* **397**, 41–43 (1999).
4. Palmer, D. M. et al. A giant γ-ray flare from the magnetar SGR 1806-20. *Nature* **434**, 1107–1109 (2005).
5. Mazets, E. P., Golentskii, S. V., Ilinskii, V. N., Aptekar, R. L. & Guryan, I. A. Observations of a flaring X-ray pulsar in Dorado. *Nature* **282**, 587–589 (1979).
6. D'Avanzo, P. Short gamma-ray bursts: a review. *J. High Energy Astrophys.* **7**, 73–80 (2015).
7. Frederiks, D. D. et al. On the possibility of identifying the short hard burst GRB 051103 with a giant flare from a soft gamma repeater in the M81 group of galaxies. *Astron. Lett.* **33**, 19–24 (2007).
8. Mazets, E. P. et al. A giant flare from a soft gamma repeater in the Andromeda Galaxy (M31). *Astrophys. J.* **680**, 545–549 (2008).
9. Svinkin, D. et al. A bright γ-ray flare interpreted as a giant magnetar flare in NGC 253. *Nature* **589**, 211–213 (2021).
10. Burns, E. et al. Identification of a local sample of gamma-ray bursts consistent with a Magnetar Giant Flare origin. *Astrophys. J. Lett.* **907**, L28–L37 (2021).
11. Trigg, A. C. et al. GRB 180128A: a second Magnetar Giant Flare candidate from the Sculptor Galaxy. Preprint at https://arxiv.org/abs/2311.09362 (2023).
12. Förster Schreiber, N. M., Genzel, R., Lutz, D. & Sternberg, A. The nature of starburst activity in M82. *Astrophys. J.* **599**, 193–217 (2003).
13. Mereghetti, S. et al. GRB 231115A: a short hard GRB detected by IBAS, positionally coincident with M82. *GRB Coord. Netw.* **35037**, 1 (2023).
14. Dalessi, S., Roberts, O. J., Veres, P., Meegan, C. & Fermi Gamma-ray Burst Monitor Team. GRB 231115A: Fermi observations of a probable Magnetar Giant Flare from M82. *GRB Coord. Netw.* **35044**, 1 (2023).
15. Cheung, C. C. et al. GRB 231115A (short): glowbug gamma-ray detection. *GRB Coord. Netw.* **35045**, 1 (2023).
16. Xue, W. C., Xiong, S. L., Li, X. B., Li, C. K. & Insight-HXMT Team. GRB 231115A: insight-HXMT/HE detection. *GRB Coord. Netw.* **35060**, 1 (2023).
17. Frederiks, D. et al. Konus-wind detection of GRB 231115A (a probable Magnetar Giant Flare from M82). *GRB Coord. Netw.* **35062**, 1 (2023).
18. Wang, Y. et al. Study the origin of GRB 231115A, short gamma-ray burst or magnetar giant flare? Preprint at https://arxiv.org/abs/2312.02848 (2023).
19. Mereghetti, S., Götz, D., Borkowski, J., Walter, R. & Pedersen, H. The INTEGRAL burst alert system. *Astron. Astrophys.* **411**, L291–L297 (2003).
20. Ubertini, P. et al. IBIS: the imager on-board INTEGRAL. *Astron. Astrophys.* **411**, L131–L139 (2003).
21. Burns, E. GRB 231115A: significance of INTEGRAL localization alignment with M82. *GRB Coord. Netw.* **35038**, 1 (2023).
22. Lebrun, F. et al. ISGRI: the INTEGRAL soft gamma-ray imager. *Astron. Astrophys.* **411**, L141–L148 (2003).

23. Labanti, C. et al. The IBIS-PICsIT detector onboard INTEGRAL. *Astron. Astrophys.* **411**, L149–L152 (2003).
24. Freedman, W. L. et al. The Hubble Space Telescope Extragalactic Distance Scale Key Project. I. The discovery of cepheids and a new distance to M81. *Astrophys. J.* **427**, 628–655 (1994).
25. Osborne, J. P. et al. GRB 231115A: Swift-XRT and Swift-UVOT observations. *GRB Coord. Netw.* **35064**, 1 (2023).
26. Rigoselli, M., Pacholski, D. P., Mereghetti, S., Salvaterra, R. & Campana, S. GRB 231115A: XMM-Newton observation. *GRB Coordinates Network* **35175**, 1 (2023).
27. Sakamoto, T. & Gehrels, N. Indication of two classes in the swift short gamma-ray bursts from the XRT X-ray afterglow light curves. In *Proc. AIP Conference on Gamma-ray Burst: Sixth Huntsville Symposium* Vol. 1133 (eds Meegan, C. et al.) 112–114 (AIP, 2009).
28. Coti Zelati, F., Rea, N., Pons, J. A., Campana, S. & Esposito, P. Systematic study of magnetar outbursts. *Mon. Not. R. Astron. Soc.* **474**, 961–1017 (2018).
29. Abbott, B. P. et al. Multi-messenger observations of a binary neutron star merger. *Astrophys. J. Lett.* **848**, L12–L70 (2017).
30. Ligo Scientific Collaboration, VIRGO Collaboration, and Kagra Collaboration. GRB 231115A: non-detection in low-latency of gravitational waves with LIGO/Virgo/KAGRA. *GRB Coord. Netw.* **35049**, 1 (2023).
31. Leroy, A. K. et al. A $z=0$ Multiwavelength galaxy synthesis. I. A WISE and GALEX atlas of local galaxies. *Astrophys. J. Supp.* **244**, 24–62 (2019).
32. Duncan, R. C. & Thompson, C. Formation of very strongly magnetized neutron stars: implications for gamma-ray bursts. *Astrophys. J. Lett.* **392**, L9–L13 (1992).
33. Cehula, J., Thompson, T. A. & Metzger, B. D. Dynamics of baryon ejection in magnetar giant flares: implications for radio afterglows, r-process nucleosynthesis, and fast radio bursts. *Mon. Not. R. Astron. Soc.* **528**, 5323–5345 (2024).
34. Frederiks, D. D. et al. Giant flare in SGR 1806-20 and its Compton reflection from the Moon. *Astron. Lett.* **33**, 1–18 (2007).
35. Mereghetti, S. et al. The first giant flare from SGR 1806-20: observations using the anticoincidence shield of the spectrometer on INTEGRAL. *Astrophys. J. Lett.* **624**, L105–L108 (2005).

Methods

INTEGRAL data analysis and results

IBIS is a γ-ray telescope based on two position-sensitive detection planes working in different overlapping energy ranges: ISGRI[22] (20 keV–1 MeV) and PICsIT[23] (175 keV–15 MeV). A coded mask placed about 3.2 m above ISGRI provides imaging capabilities over a field of view of roughly 30 × 30 degrees^2. GRB 231115A was detected at an off-axis angle of 4°, inside the fully coded field of view. For the data reduction and analysis, we used v.11.2 of the Offline Science Analysis software[36], with the most recent calibration files, that properly account for the time evolution of the instrument response.

Burst spectrum. We extracted an ISGRI spectrum, in 14 logarithmically spaced energy channels between 30 and 500 keV, for the time interval from 15 h 36 min 20.687 s to 15 h 36 min 20.748 s UT. The PICsIT spectrum for the same time interval was extracted from the spectral-timing data mode in eight predefined energy channels spanning 212–2,600 keV. Data in spectral-timing mode (counts integrated over the whole detector in 3.9 ms time bins) do not provide imaging information (contrary to the ISGRI data). Therefore, the background count rate in each PICsIT energy channel was calculated as the median count rate during the INTEGRAL pointing (5,013 s duration) containing the burst. A proper correction factor was applied to the PICsIT effective area to account for the angular distance between the IBIS pointing direction and GRB 231115A.

We added 5% systematic uncertainties to both spectra. The ISGRI and PICsIT spectra were fitted simultaneously using XSPEC[37] v.12.12.1. A fit with a power law was unacceptable ($\chi^2 = 59.4$ for 17 degrees of freedom), whereas a power law with exponential cut-off, defined as $F(E) = KE^{\alpha}\exp(-E(2+\alpha)/E_p)$, gave a good fit with photon index $\alpha = 0.04^{+0.27}_{-0.24}$, peak energy $E_p = 551^{+81}_{-59}$ keV and 30–2,600 keV flux $F = (7.2^{+0.6}_{-0.7}) \times 10^{-6}$ erg cm^{-2} s^{-1}.

The ISGRI spectrum for the time interval corresponding to the whole GRB, from 15 h 36 min 20.687 s to 15 h 36 min 20.833 s UT, is less well constrained, but the best fit parameters are within the errors consistent with those of the ISGRI plus PICsIT spectrum. All the fit parameters are summarized in Extended Data Table 1, in which we also give the results obtained with a blackbody model.

Follow-up observation. Immediately after the discovery of GRB 231115A we requested an INTEGRAL ToO observation that started only 21 h after the burst and continued in the next satellite revolution. The first part of the ToO was done between 12 h 38 min and 19 h 46 min UT of 16 November. The next one from 07 h 21 min UT of 17 November to 23 h 09 min UT of 18 November, resulting in a total exposure of 162 ks divided in 57 pointings. Using the Offline Science Analysis v.11.2 software, we produced the mosaics of the ISGRI images in the 30–100 keV energy range for three periods: 16 November, 17–18 November and 16–18 November. No sources were detected at the position of GRB 231115A. The 3σ upper limits on the 30–100 keV flux, derived assuming a thermal bremsstrahlung spectrum with temperature $kT = 30$ keV, are 6.5×10^{-11} erg cm^{-2} s^{-1} for 16 November, 2.9×10^{-11} erg cm^{-2} s^{-1} for 17–18 November and 2.6×10^{-11} erg cm^{-2} s^{-1} for the sum of the two periods. We also derived an upper limit of 3.8×10^{-10} erg cm^{-2} s^{-1} on the flux in the time interval from $T_0 + 1.7$ s to $T_0 + 11.8$ min, during which the GRB 231115A position was in the IBIS field of view. All these upper limits are plotted in Fig. 3, which shows that even a giant flare as energetic as the one emitted from SGR 1806–20 at the distance of M82 would have been undetectable by IBIS after the initial bright pulse.

Search for past activity from M82. The region of M82 has been repeatedly observed with INTEGRAL, starting in November 2003. After eliminating the time intervals with strong and variable background (typically due to solar activity or to particles trapped in the Earth radiation belts when the satellite is close to perigee) we obtained about 16 millions of seconds of useful time with M82 in the IBIS field of view. We extracted ISGRI light curves in the 30–150 keV energy range, using only detector pixels illuminated for more than 50% from a source at the GRB 231115A position and searched for excess counts in the light curves over eight logarithmically spaced timescales between 0.01 and 1.28 s (see ref. 38 for more details). All the burst candidates found in the light curves were then examined by making sky images of the corresponding time intervals. None of them showed the presence of a source at the M82 position. Through simulations, we found that bursts down to a factor of roughly five fainter than GRB 231115A would have been detected in these data, assuming the same time profile and spectrum.

X-ray observations

Swift pointed at M82 and started to collect data 9.0 ks after the burst occurrence[25]. Swift–XRT observations were carried out in Photon Counting mode in the 9.0–39.2 ks time interval, collecting 4.4 ks of data. No new X-ray sources were detected within the INTEGRAL error region of GRB 231115A. The 3σ upper limit is position dependent due to the diffuse X-ray emission from the M82 galaxy. Outside the galaxy, the upper limit on the count rate is roughly $2–3 \times 10^{-3}$ counts per s. Assuming a power-law spectrum with photon index $\Gamma = 2$ and the galactic column density of 6.5×10^{20} cm^{-2} (the total galactic absorption column in the line of sight of M82 (ref. 39)) this corresponds to a 0.3–10 keV unabsorbed flux of roughly 10^{-13} erg cm^{-2} s^{-1}.

A 47-ks-long ToO observation of GRB 231115A was carried out with the XMM-Newton satellite, starting on 16 November 2023 at 08 h 29 min 16 s UT, about 16.9 h after the burst (observation ID 093239)[26]. The EPIC-pn[40] and the two EPIC-MOS[41] cameras were operated in Full window mode, with the thin optical-blocking filter. We processed the data with the EPPROC and EMPROC pipelines of v.8 of the Science Analysis System[42] and the most recent calibration files and selected the EPIC events with standard filtering expressions. Time intervals of high background were removed with the ESPFILT task with standard parameters, thus yielding net exposure times of 7.56 ks (pn), 18.78 ks (MOS1) and 23.41 ks (MOS2). We selected single- and multiple-pixel events (PATTERN ≤ 4 for the pn and less than or equal to 12 for the MOS cameras); out-of-time events were also removed following the standard procedure[43].

Extended Data Fig. 1 shows the pn exposure-corrected images in the soft (0.3–2.0 keV) and hard (2–10 keV) energy ranges. The images are dominated by the diffuse X-ray emission of the M82 galaxy, especially in the soft X-ray band. We compared the images obtained in this observation with those of all the previous pointings on M82 available in the XMM-Newton archive (observation IDs 011229, 020608, 056059, 065780, 087094, 089106). We did not find any evidence for the appearance of a new source. In our observation, the total emission between 2 and 10 keV from a circular region of radius 1.5 arcmin at the centre of the galaxy (coordinates RA 09 h 55 min 50.9 s, dec. +69° 40′ 47″; J2000) can be described by an absorbed power law with $N_H = (1.0 \pm 0.1) \times 10^{22}$ cm^{-2}, photon index $\Gamma = 2.01 \pm 0.04$ and unabsorbed flux $F_{2–10\,keV} = (2.88 \pm 0.04) \times 10^{-11}$ erg cm^{-2} s^{-1}. The flux measured in previous XMM-Newton observations from the same extraction region and the same spectral model varied between roughly 1.2×10^{-11} and 5.4×10^{-11} erg cm^{-2} s^{-1}, indicating the presence of one or more variable sources that cannot be individually resolved with the XMM-Newton spatial resolution.

To compute the upper limit for a new point source in the GRB 231115A error box, we applied the EUPPER task to the 2–10 keV images. We used a circle of radius 15″ for the source extraction and a concentric annulus of radii 22.5″ and 30″ for the background. The derived upper limits have been corrected for the fraction of source counts falling outside the extraction circle. Extended Data Fig. 2 shows the 3σ upper limits obtained by applying this procedure on a grid of positions with a step of 5″.

We used the appropriate EPIC response matrices to convert the count rates of each camera to fluxes in the 0.3 and 2–10 keV energy ranges, with the assumption of an absorbed power-law spectrum with photon index $\Gamma = 2$ and $N_H = 6.5 \times 10^{20}$ cm^{-2}. Finally we combined the upper limits

of the three cameras to obtain an EPIC upper limit for each energy band. The results are shown in Extended Data Fig. 3. About 60% of the error circle has a 3σ upper limit of $F_{2-10\,\mathrm{keV}} = 1.2 \times 10^{-14}$ and $F_{0.3-10\,\mathrm{keV}} = 4.0 \times 10^{-14}$ erg cm^{-2} s^{-1}. In less than 10% of the error circle, the upper limit is worse than 7×10^{-14} erg cm^{-2} s^{-1} (2–0 keV) and 1.6×10^{-13} erg cm^{-2} s^{-1} (0.3–10 keV). At the distance of M82, these fluxes correspond to luminosities of 1.9×10^{36} and 6.2×10^{36} erg s^{-1}, respectively.

Extended Data Fig. 4 shows the comparison between the X-ray light curves of short GRBs (defined such as $T_{90} \leq 2$ s), obtained from the Swift GRB catalogue[44] and the 3σ upper limits we derived from the Swift and XMM-Newton observations of GRB 231115A.

Optical observations

Multi-filter follow-up optical observations of GRB 231115A were carried out with the wide-field Schmidt telescopes sited in the INAF observatories of Padova (Asiago, Italy), Abruzzo (Campo Imperatore, Italy) and with the 3.6 m Telescopio Nazionale Galileo (TNG, Canary Islands, Spain) between about 5 and 12 h from the event T_0. We also took more images in the V, R, and I bands about 7 h after T_0 with the 120 cm Newton telescope located at the Observatoire de Haute Provence (OHP, France). The log of the observations is reported in Extended Data Table 2. Image reduction was carried out following the standard procedures: subtraction of an averaged bias frame and division by a normalized flat frame. Astrometry was performed using the Pan-STARRS[45] catalogue. We carried out image subtraction with respect to SDSS[46] and telescope archival templates using the HOTPANTS (High Order Transform of Psf ANd Template Subtraction code[47]) package to find and pinpoint variable sources within the INTEGRAL error circle. Aperture and PSF-matched photometry were performed using the DAOPHOT package[48] and the STDPipe[49] and the photutils[50,51] packages for OHP/T120 images. To minimize any systematic effect, we performed differential photometry with respect to a selection of local isolated and non-saturated reference stars from the Pan-STARRS[45]. The presence of the M82 galaxy makes the background highly non-uniform within the INTEGRAL error circle. Magnitude upper limits have been computed for two regions (Extended Data Table 2): one (most conservative) corresponding to the centre of the M82 galaxy (RA 09 h 55 min 53.75 s, dec. +69° 40′ 53.9″; J2000) and another outside the core of the galaxy light (RA 09 h 56 min 11.31 s, dec. +69° 39′ 09.6″; J2000).

Our upper limits in the optical bands (Extended Data Table 2) exclude most cosmological short GRB afterglows. If these occurred at the distance of M82, in a position located inside (outside) the galaxy, a short GRB would have produced an optical afterglow more than 12 (16) magnitudes brighter than our limits (Extended Data Fig. 6). These upper limits are about nine (thirteen) magnitudes fainter than the expected brightness of a kilonova such as AT2017gfo occurring at the distance of M82 inside (outside) the galaxy. Because kilonovae associated to short GRBs can show significant differences in their luminosity, spectral properties and temporal evolution[52], we simulated a set of light curves with the POSSIS code[53] using the parameter range reported in ref. 54. We found that even the faintest event, placed at the distance of M82, is still about five (nine) magnitudes brighter than our upper limits.

Data availability

The data of the INTEGRAL, XMM-Newton and Swift satellites are publicly available in the respective online archives (https://www.isdc.unige.ch/integral/archive, https://www.cosmos.esa.int/web/xmm-newton/xsa, https://swift.gsfc.nasa.gov/archive/). Optical data are available upon request.

Code availability

The software used for the data analysis is public and can be retrieved at https://www.cosmos.esa.int/web/xmm-newton/sas, https://www.isdc.unige.ch/integral/analysis#Software, https://heasarc.gsfc.nasa.gov/xanadu/xspec/.

36. Goldwurm, A. et al. The INTEGRAL/IBIS scientific data analysis. *Astron. Astrophys.* **411**, L223–L229 (2003).
37. Arnaud, K. A. XSPEC: the first ten years. In *Proc. Astronomical Data Analysis Software and Systems V* Vol. 101 (eds Jacoby, G. H. & Barnes, J.) 17–20 (ASP, 1996).
38. Mereghetti, S., Topinka, M., Rigoselli, M. & Götz, D. INTEGRAL limits on past high-energy activity from FRB 20200120E in M81. *Astrophys. J. Lett.* **921**, L3–L7 (2021).
39. HI4PI Collaboration. HI4PI: a full-sky H I survey based on EBHIS and GASS. *Astron. Astrophys.* **594**, A116 (2016).
40. Strüder, L. et al. The European Photon Imaging Camera on XMM-Newton: the pn-CCD camera. *Astron. Astrophys.* **365**, L18–L26 (2001).
41. Turner, M. J. L. et al. The European Photon Imaging Camera on XMM-Newton: the MOS cameras. *Astron. Astrophys.* **365**, L27–L35 (2001).
42. Gabriel, C. et al. The XMM-Newton SAS—distributed development and maintenance of a large science analysis system: a critical analysis. In *Proc. Astronomical Data Analysis Software and Systems (ADASS) XIII* Vol. 314 (eds Ochsenbein, F. et al.) 759–763 (ASP, 2004).
43. European Space Agency. Dealing with epic out-of-time (OOT) events. *XMM-Newton* www.cosmos.esa.int/web/xmm-newton/sas-thread-epic-oot (2023).
44. NASA. Swift GRBS, look up a burst. *Goddard Space Flight Center* http://swift.gsfc.nasa.gov/archive/grb_table (2023).
45. Mulgrew, P. Pan-STARRS1 data archive. *Space Telescope Science Institute* http://outerspace.stsci.edu/display/PANSTARRS/ (2022).
46. SDSS. *SDSS-V: pioneering panoptic spectroscopy* www.sdss.org (2022).
47. Becker, A. HOTPANTS: high order transform of PSF and template subtraction. ascl:1504.004 (Astrophysics Source Code Library, 2015).
48. Stetson, P. B. DAOPHOT: a computer program for crowded-field stellar photometry. *Pub. Ast. Soc. Pac.* **99**, 191–222 (1987).
49. Karpov, S. STDPipe: simple transient detection pipeline. ascl:2112.006 (Astrophysics Source Code Library, 2021).
50. Bradley, L. et al. astropy/photutils: 1.1.0. *Zenodo* https://doi.org/10.5281/zenodo.4624996 (2021).
51. astropy, photoutils v.1.11.0. *GitHub* http://github.com/astropy/photutils (2024).
52. Rossi, A. et al. A comparison between short GRB afterglows and kilonova AT2017gfo: shedding light on kilonovae properties. *Mon. Not. R. Astron. Soc.* **493**, 3379–3397 (2020).
53. Bulla, M. POSSIS: predicting spectra, light curves, and polarization for multidimensional models of supernovae and kilonovae. *Mon. Not. R. Astron. Soc.* **489**, 5037–5045 (2019).
54. Ferro, M. et al. A search for the afterglows, kilonovae, and host galaxies of two short GRBs: GRB 211106A and GRB 211227A. *Astron. Astrophys.* **678**, A142–A162 (2023).

Acknowledgements We thank the ESA Mission Scientists J.-U. Ness and N. Schartel for approving and quickly implementing the INTEGRAL and XMM-Newton ToO observations. This work is based on observations with INTEGRAL and XMM-Newton, ESA missions with instruments and science data centres funded by ESA member states, and with the participation of the Russian Federation and the United States. It is also based on observations made with the Italian TNG operated on the island of La Palma by the Fundación Galileo Galilei of the INAF (Istituto Nazionale di Astrofisica) at the Spanish Observatorio del Roque de los Muchachos of the Instituto de Astrofisica de Canarias. This paper includes optical data taken with the Schmidt 67/92 telescope operated by INAF Osservatorio Astronomico di Padova (Mount Ekar, Asiago). This work received financial support from INAF through the Magnetars Large Program Grant (Principal Investigator S.M.) and from the GRAWITA Large Program Grant (Principal Investigator P.D.A.). J.C.R., A.B., S.M. and P.U. acknowledge financial support from ASI under contract no. 2019-35-HH.0. F.O. acknowledges support from MIUR, PRIN 2020 (grant no. 2020KB33TP) 'Multimessenger astronomy in the Einstein Telescope Era' (METE). J.C.R. acknowledges support from the European Union's Horizon 2020 Programme under the AHEAD2020 project (grant agreement no. 871158). P.D.A. and S.C. acknowledge funding from the Italian Space Agency, contract ASI/INAF no. I/004/11/4.

Author contributions All authors reviewed the manuscript and contributed to the source interpretation. S.M. coordinated the work and the interpretation of the results, contributed to the analysis of the INTEGRAL and XMM-Newton data, and wrote most of the manuscript. R.S. and E.A. contributed to write the main part of the paper. D.P.P. and J.C.R. carried out most of the INTEGRAL data analysis. D.G., C.F., E.B., L.D. and V.S. routinely contribute to the operation of the IBAS software and participated to the near real time INTEGRAL analysis. P.D.A. coordinated the analysis of the optical data from Italian telescopes. M.R. analysed the XMM-Newton data and contributed to the INTEGRAL spectral analysis. S.C. analysed the Swift data. M.T. contributed to the software for the burst search in archival data. D.T., W.T., D.S. and C.A. coordinated the observation and the analysis of the optical data taken at OHP. L.T. analysed the optical data taken with the Schmidt 67/92 telescope in Asiago under the Large Program 'Search and characterization of optical counterparts of GW triggers' (P.I. Tomasella). A.R. and E.C. triggered, reduced and analysed the observations at the Asiago Schmidt telescope. R.B. and M.F. provided the short GRB afterglows and kilonovae observed and simulated optical light curves.

Competing interests The authors declare no competing interests.

Additional information
Correspondence and requests for materials should be addressed to Sandro Mereghetti.

Peer review information *Nature* thanks Eric Burns and David Palmer for their contribution to the peer review of this work.

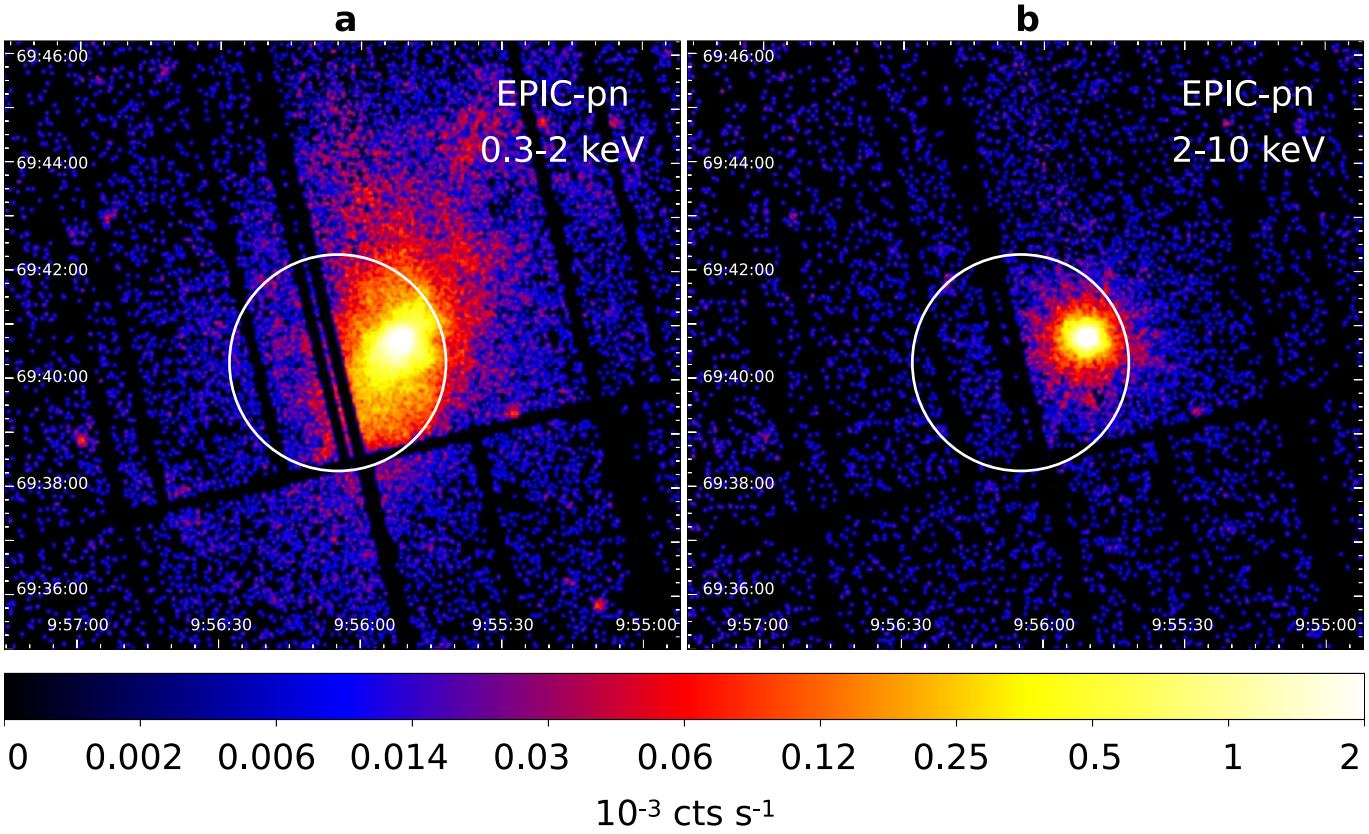

Extended Data Fig. 1 | EPIC-pn images of M82. The exposure-corrected images refer to the 0.3–2 keV (**a**) and 2–10 keV (**b**) energy ranges. The 90% c.l. error circle of GRB 231115A has a radius of 2 arcmin.

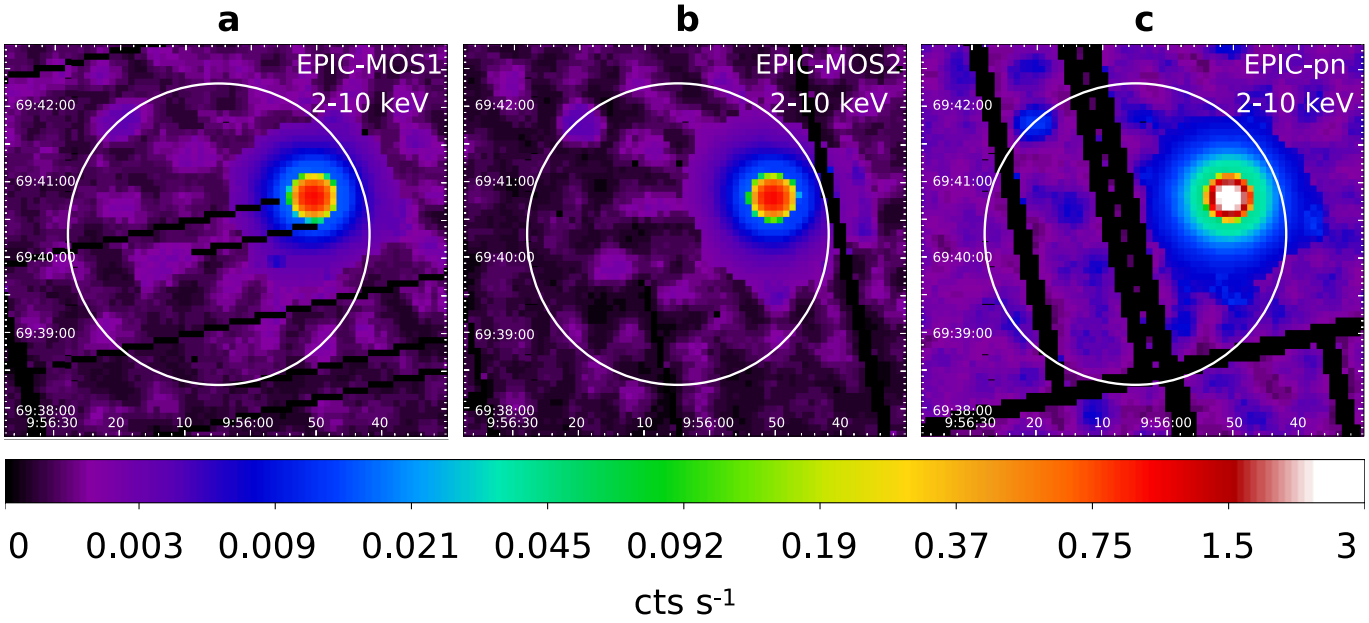

Extended Data Fig. 2 | Maps of count rate upper limits. The figure gives 3-σ upper limits on the 2–10 keV count rates of the EPIC-MOS1 (**a**), EPIC-MOS2 (**b**) and EPIC-pn (**c**) cameras. The 90% c.l. error circle of GRB 231115A has a radius of 2 arcmin.

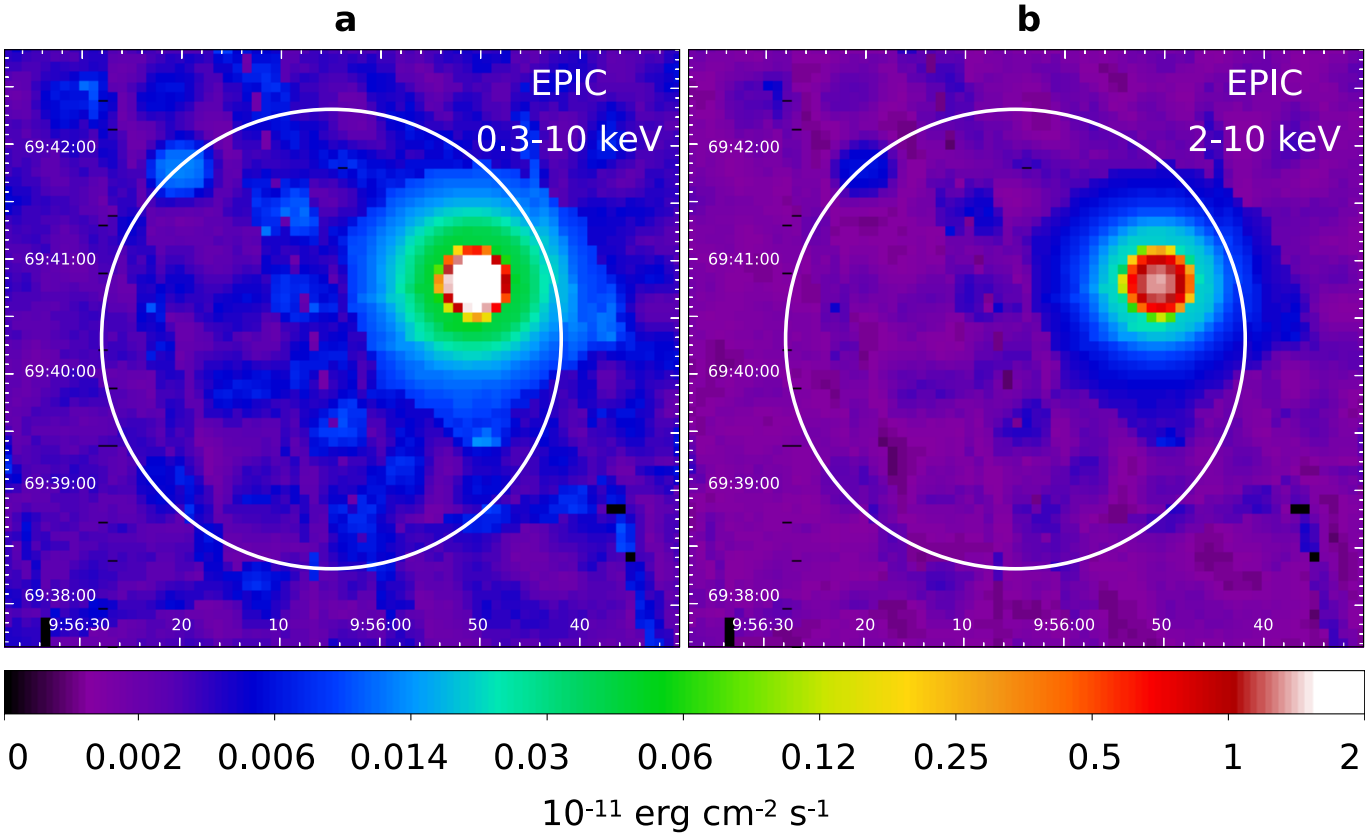

Extended Data Fig. 3 | Maps of flux upper limits. The figure gives 3-σ upper limits on the fluxes in the 2–10 keV (**a**) and 0.3–10 keV (**b**) energy range, obtained by combining the three maps of Extended Data Fig. 2. The 90% c.l. error circle of GRB 231115A has a radius of 2 arcmin.

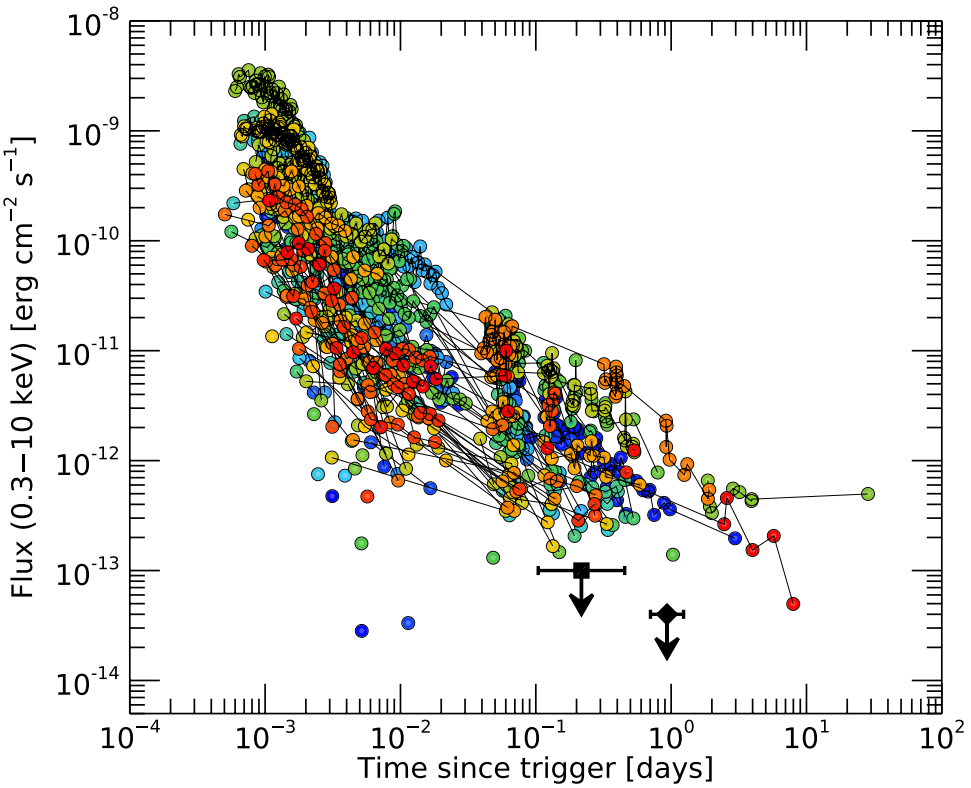

Extended Data Fig. 4 | X-ray light curves of short GRB afterglows. The *Swift*/XRT (black square) and *XMM-Newton*/EPIC (black diamond) 3-σ upper limits of GRB 231115A are indicated.

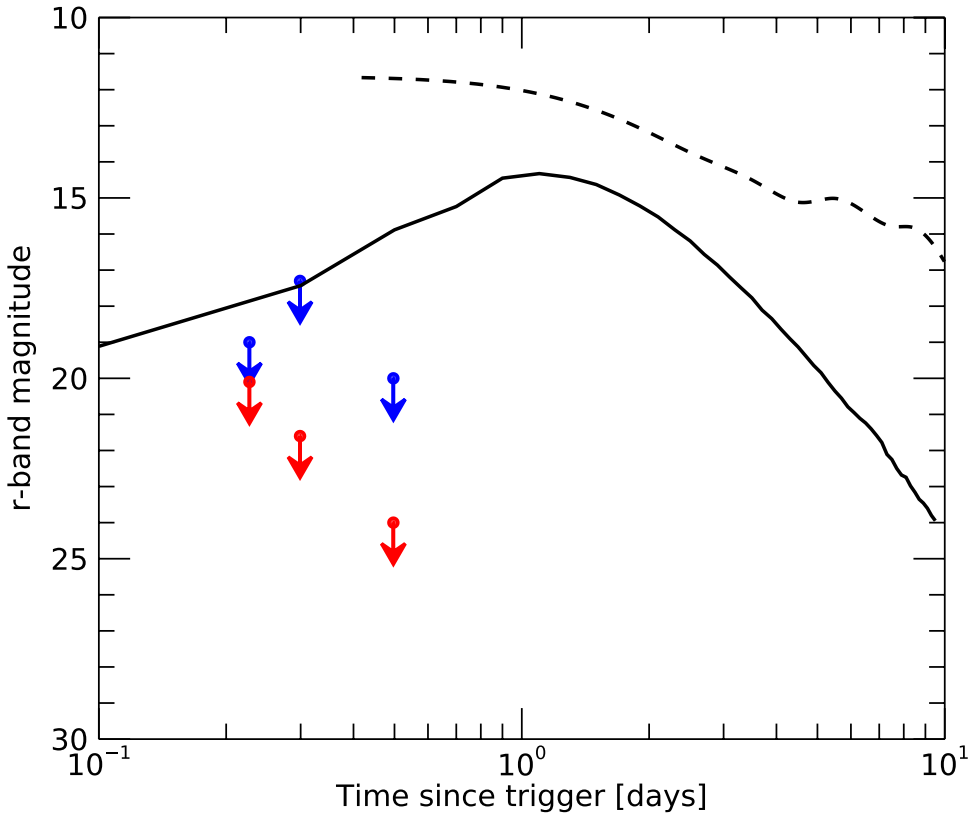

Extended Data Fig. 5 | Optical light curves of kilonovae. The r-band light curves of AT2017gro and of the faintest red kilonova (simulated with the POSSIS code) are shown with dashed and solid lines, respectively, assuming the M82 distance (3.6 Mpc). The magnitude 3-σ upper limits obtained for a position inside (outside) the M82 galaxy are shown as blue (red) arrows.

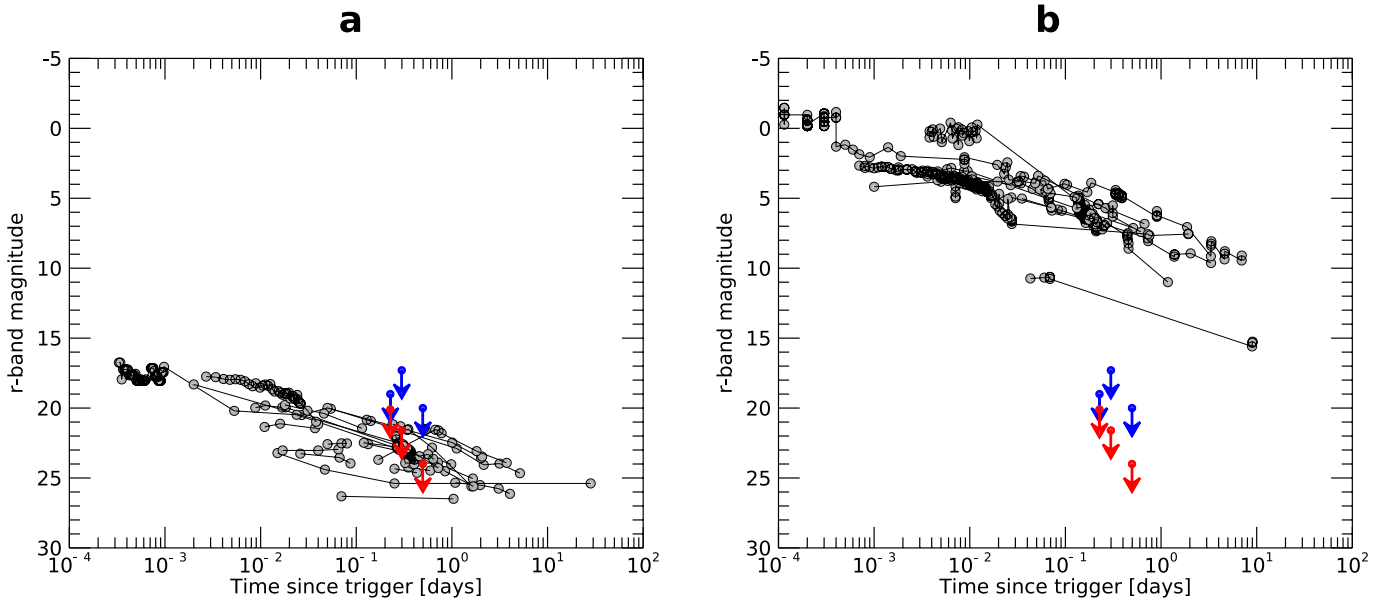

Extended Data Fig. 6 | Optical light curves of short GRB afterglows. The observed light curves are shown in **a**, while **b** shows the light curves of those GRBs which have a measure of redshift, rescaled to the M82 distance (3.6 Mpc). The 3-σ upper limits obtained for a position inside (outside) the M82 galaxy are shown as blue (red) arrows.

Extended Data Table 1 | Results of spectral fits of GRB 231115A

Detectors	ISGRI+PICsIT	ISGRI
Time interval	0.687–0.748	0.687–0.833
Blackbody		
kT (keV)	108^{+7}_{-5}	68^{+12}_{-11}
Flux (10^{-6} erg cm^{-2} s^{-1})	$7.9^{+0.6}_{-0.7}$	$2.1^{+0.6}_{-0.7}$
χ^2 / d.o.f.	$31.9/17$	$16.4/12$
Cut-off power law		
α	$0.04^{+0.27}_{-0.24}$	$0.55^{+0.50}_{-0.42}$
E_p (keV)	551^{+81}_{-59}	355^{+158}_{-89}
Flux (10^{-6} erg cm^{-2} s^{-1})	$7.2^{+0.6}_{-0.7}$	2.7 ± 1.1
χ^2 / d.o.f.	$17.2/16$	$14.9/11$

Errors are at 1σ, fluxes are in the 30–2600 keV energy range. Time intervals are in seconds after T_0 = 15:36:20 UT.

Extended Data Table 2 | Log of optical observations of GRB 231115A

UT observation (start - stop)	Exposure (s)	T - T_0 (days)	Telescope	Magnitude	Filter
2023-11-15 20:40:03 - 20:54:15	5×180 s	0.211	Asiago	$> 19.1 (> 20.1)$	g
2023-11-15 20:54:59 - 21:12:11	5×180 s	0.221	Asiago	$> 19.0 (> 20.1)$	r
2023-11-15 21:12:45 - 21:27:45	5×180 s	0.234	Asiago	$> 18.3 (> 19.8)$	i
2023-11-15 21:38:00 - 22:16:30	7×300 s	0.251	Campo Imperatore	$> 14.8 (> 18.9)$	z
2023-11-15 22:38:25 - 21:31:30	9×300 s	0.293	Campo Imperatore	$> 16.5 (> 19.8)$	i
2023-11-15 23:33:32 - 21:38:00	7×300 s	0.331	Campo Imperatore	$> 18.8 (> 20.7)$	g
2023-11-15 22:35:32 - 22:57:23	1×1400 s	0.299	OHP	$> 17.3 (> 21.6)$	r
2023-11-15 23:04:02 - 23:14:02	1×600 s	0.314	OHP	$> 18.0 (> 22.0)$	g
2023-11-15 23:14:30 - 23:19:30	1×300 s	0.320	OHP	$> 17.1 (> 20.1)$	i
2023-11-16 03:25:04 - 03:38:16	5×120 s	0.492	TNG	$> 20.0 (> 24.0)$	r
2023-11-16 03:40:24 - 03:59:09	7×120 s	0.503	TNG	$> 18.9 (> 23.8)$	i
2023-11-16 04:00:28 - 04:19:17	7×120 s	0.530	TNG	$> 18.7 (> 22.7)$	z

Magnitudes are in the AB system, not corrected for Galactic extinction. Upper limits are given at 3-σ confidence level for a source within (outside) the M82 galaxy.